# Conformational Analysis of Octopamine and Synephrine in the Gas Phase

**ARTICLE** *in* THE JOURNAL OF PHYSICAL CHEMISTRY A · MAY 2013

Impact Factor: 2.69 · DOI: 10.1021/jp4032223 · Source: PubMed



**8 AUTHORS**, INCLUDING:

Carlos Cabezas
Universidad de Valladolid
**50** PUBLICATIONS **361** CITATIONS
SEE PROFILE

Celina Bermúdez
Universidad de Valladolid
**11** PUBLICATIONS **102** CITATIONS
SEE PROFILE

Santiago Mata
Universidad de Valladolid
**47** PUBLICATIONS **762** CITATIONS
SEE PROFILE

Rui Fausto
University of Coimbra
**330** PUBLICATIONS **4,520** CITATIONS
SEE PROFILE

THE JOURNAL OF PHYSICAL CHEMISTRY A

Article

pubs.acs.org/JPCA

# Conformational Analysis of Octopamine and Synephrine in the Gas Phase

Carlos Cabezas,[†] Alcides Simão,[‡] Celina Bermúdez,[†] Marcelino Varela,[†] Isabel Peña,[†] Santiago Mata,[†] Rui Fausto,[‡] and José Luis Alonso*[,†]

[†]Grupo de Espectroscopia Molecular (GEM), Unidad Asociada CSIC, Edificio Quifima, Laboratorios de Espectroscopia y Bioespectroscopia, Universidad de Valladolid, 47005 Valladolid, Spain

[‡]Department of Chemistry, University of Coimbra, P-3004-535 Coimbra, Portugal

Supporting Information

**ABSTRACT:** Four and six conformers of the neurotransmitters octopamine and synephrine, respectively, have been identified in the gas phase using a laser ablation device in combination with a molecular-beam Fourier transform microwave spectrometer operating in the 4−10 GHz frequency range. The identification of all of the conformers was based on a comparison of the experimental rotational and $^{14}N$ quadrupole coupling constants with those predicted by ab initio calculations, as well as the relative values of their electric dipole moment components. The conformational preferences have been rationalized in terms of the various intramolecular forces operating in the different conformers of the studied molecules. All observed species are characterized by an intramolecular hydrogen bond of the type O−H···N established in the side chain of the neurotransmitters, which adopts an extended disposition in their most stable forms. For conformers with a folded side chain, an extra N−H···$\pi$ hydrogen-bond-type interaction is established between the amino group and the $\pi$ system of the aromatic ring.

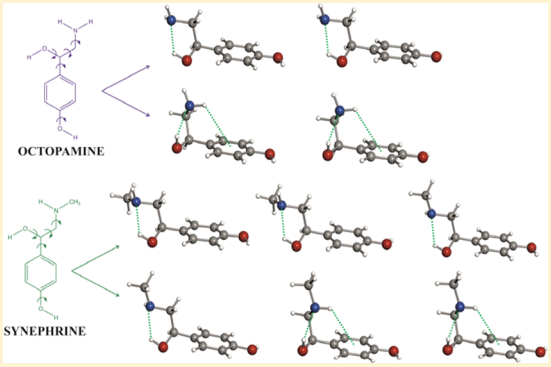


## INTRODUCTION

Neurotransmitters are substances produced and secreted by a neuron to cross the synapse space between neurons. They comprise several different families of compounds, including amino acids, peptides, and biogenic amines. A key structural feature of neurotransmitters is their high conformational flexibility. This dictates molecular shape, which, in turn, has a great influence on both transport properties and molecular recognition processes at the receptor site.[1]

The study of the intricate processes of neurotransmission at the molecular level and the interactions of neurotransmitters under complex biological conditions must be preceded by detailed characterization of the conformational properties of the neurotransmitters in the absence of intermolecular interactions, thus avoiding alterations of their intrinsic structural preferences, matching the conditions found in the gas phase. However, pure neurotransmitters at room temperature normally present themselves as solids with low to very low vapor pressures and high melting points. Hence, the question of how to efficiently populate the gas phase with these compounds is a critical one for the success of these investigations. Conventional heating methods can be used to achieve the necessary amount of compound in the gas phase, but they are useful for only a handful of these compounds, easily vaporizable neurotransmitters. Combining molecular-beam Fourier transform microwave (MB-FTMW) spectroscopy with heating methods, we have characterized the conformational panoramas of several neurotransmitters in the gas phase, including 2-phenylethylamine,[2] *p*-methoxyphenylethylamine,[3] norephedrine, ephedrine, and pseudoephedrine.[4] However, the investigation of a complete series of neurotransmitters by MB-FTMW spectroscopy is not possible because of the high melting points and associated very low vapor pressures of these compounds. In these cases, laser ablation has been shown to be an efficient method for vaporizing solid samples without the decomposition problems encountered using heating methods. Indeed, laser ablation in combination with molecular beams and microwave spectroscopy (LA-MB-FTMW spectroscopy)[5] has proven to be a powerful tool in the investigation of the gas-phase conformational behavior of solid neurotransmitters such as taurine,[6] tryptamine,[7] $\gamma$-aminobutyric acid (GABA),[8] serotonin,[9] and dopamine.[10]

In a continuation of our ongoing investigation of the conformations of neurotransmitters in the gas phase using rotational spectroscopy, in the present study, we considered octopamine [4-(2-amino-1-hydroxyethyl)phenol] and synephrine {4-[1-hydroxy-2-(methylamino)ethyl]phenol} as target compounds. These molecules (see Figures 1 and 2) are

**Received:** April 1, 2013
**Revised:** May 14, 2013
**Published:** May 15, 2013

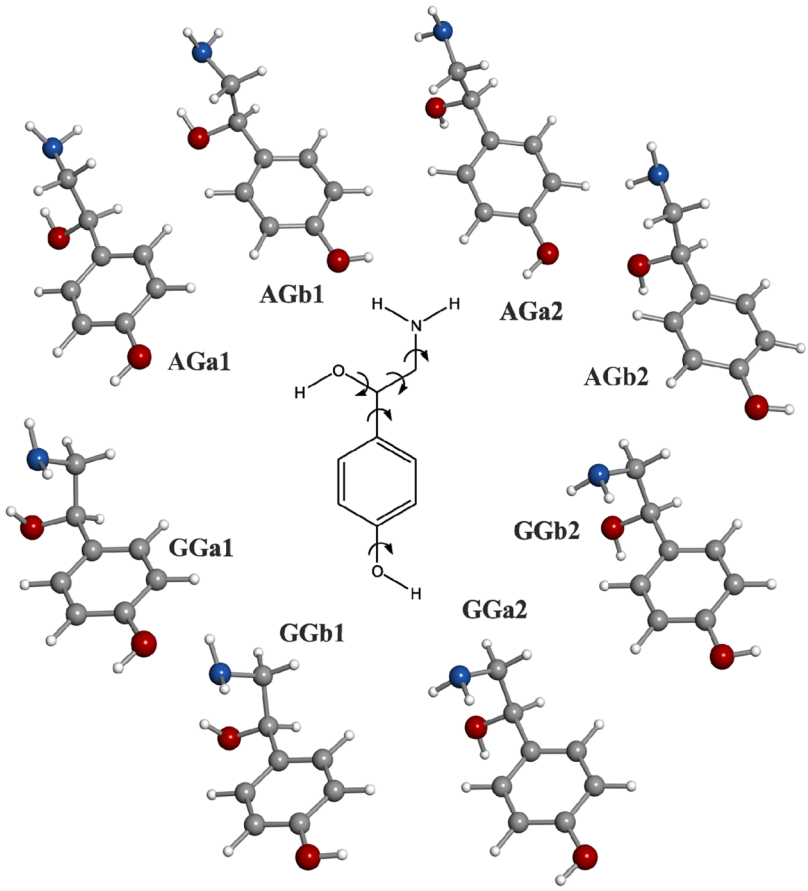


**Figure 1.** Eight lowest-energy conformers of octopamine predicted by ab initio calculations. The sketch in the center indicates the hindered single-bond rotations that govern conformational equilibrium.

endogenous biogenic amines that have been shown to act as important neurotransmitters. Octopamine is the equivalent of norepinephrine in insects and has been implicated in regulating aggression in invertebrates, with different effects on different species.[11] On the other hand, synephrine is a naturally occurring alkaloid in many cactus and citrus juice fruits[12] that is commonly marketed as a weight-loss drug, acting as a stimulant in humans.[13] As far as we could ascertain in the literature, no previous studies have been reported on the conformational preferences of octopamine, whereas synephrine was studied using a combination of electronic and IR dip spectroscopy techniques.[14] The two related systems 2-amino-1-phenylethanol (APE) and 2-methylamino-1-phenylethanol (MAPE), without the phenolic OH group in the para position, were studied[15] by free-jet absorption microwave spectroscopy.

On this basis, we undertook the problem of characterizing the conformational preferences of octopamine and synephrine and the nature of the intramolecular interactions that determine these preferences, taking advantage of the high resolution of LA-MB-FTMW spectroscopy. The obtained results allowed us to conclusively identify four conformers of octopamine and six conformers of synephrine. The role of intramolecular hydrogen-bonding interactions is discussed in terms of the stabilization of all of the observed conformers.

## EXPERIMENTAL AND COMPUTATIONAL METHODS

**Experimental Setup.** A laser ablation molecular-beam Fourier transform microwave (LA-MB-FTMW) spectrometer that operates in the 4−10 GHz frequency range, described elsewhere,[5] was used to record the rotational spectra of both studied molecules. Solid rods of fine-powdered octopamine (Interchim, 95%, mp = 169−171 °C) or synephrine (Sigma-Aldrich, 98%, mp = 187 °C) were mixed with minimum quantities of a commercial binder to form a cylindrical rod. The samples were then vaporized using the third harmonic (355 nm) of a Nd:YAG picosecond laser (20-ps pulse length) at energies of ∼13 mJ/pulse. The neutral vaporized molecules were seeded in the carrier gas (Ne, 15 bar) and expanded into a Fabry−Pérot resonator. After the microwave pulses had been sent through the cavity, the emission free induction decay of the molecules was recorded in the time domain and Fourier transformed to yield the frequency-domain spectrum. Because the supersonic jet and the microwave resonator axis were positioned collinearly, signals appeared split into Doppler doublets (see Figures 3 and 5). The arithmetic mean of the doublets was taken as the final frequency. The estimated accuracy of the frequency measurements is better than 3 kHz.

**Ab Initio Calculations.** Ab initio calculations were performed to guide the identification of the species detected in the supersonic expansion. The calculations were performed at the MP2/6-311++G(d,p) level of theory, using the Gaussian 09[16] suite of programs. Eight conformers for octopamine and 12 conformers for synephrine (depicted in Figures 1 and 2, respectively) were found in an energy window of 800 $cm^{-1}$ above the global minimum for each compound. In this article, each conformer of octopamine is specified by a combination of four symbols: a pair of capital letters indicating the orientations


dx.doi.org/10.1021/jp4032223 | J. Phys. Chem. A 2013, 117, 4907−4915

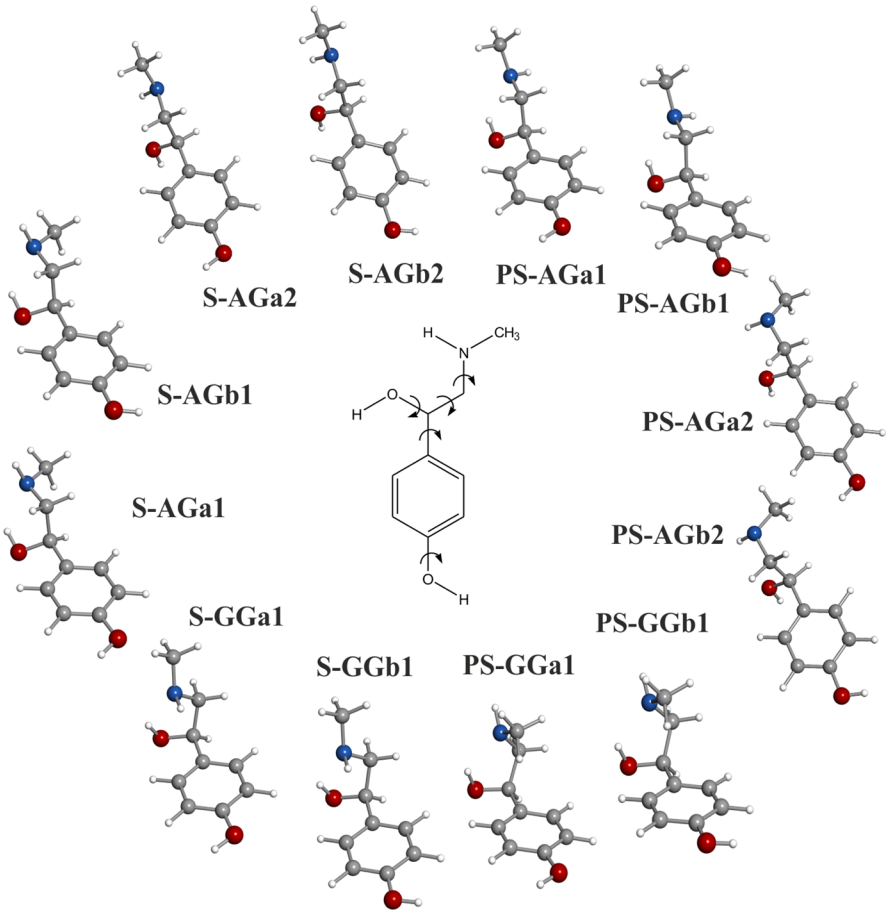


**Figure 2.** Twelve lowest-energy conformers of synephrine predicted by ab initio calculations. The sketch in the center indicates the hindered single-bond rotations that govern conformational equilibrium.

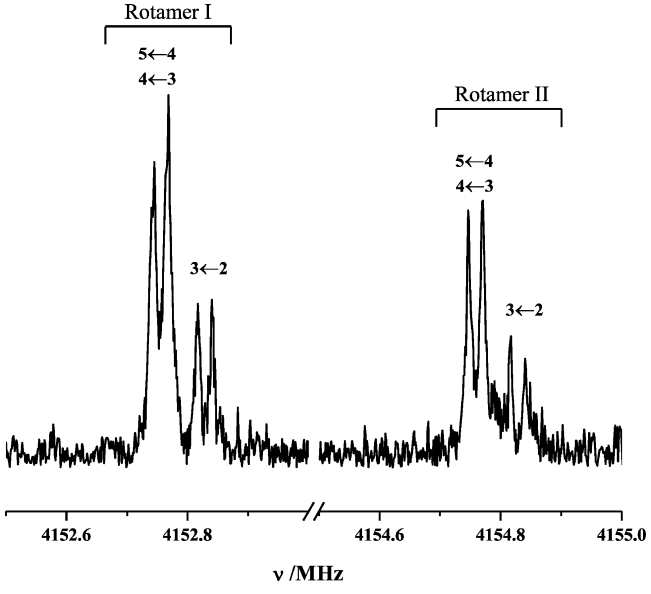


**Figure 3.** $4_{04}-3_{03}$ rotational transitions of rotamers I and II of octopamine, illustrating the hyperfine structure patterns arising from the $^{14}N$ nuclear quadrupole coupling interactions. The hyperfine components that appear as doublets due to the Doppler effect are labeled with the quantum numbers F′ ← F″.

of the $CC_\alpha C_\beta N$ and $OC_\alpha C_\beta N$ chains, for example, AG or GG (where A and G represent anti and gauche arrangements, respectively); subscripts a and b specifying the different orientations of the OH group of the ring; and subscripts 1 and 2 designating the increasing order in energy. Synephrine differs from octopamine by the presence of a methyl group in the amino group, substituting for a hydrogen atom. The presence of this methyl group induces chirality at the nitrogen atom, thus giving rise to two distinct forms: synephrine (S) and pseudosynephrine (PS). Hence, in the designation of the conformers of synephrine, a prefix of S or PS is used to distinguish between the two possible configurations of the amino group. The predicted rotational constants, $^{14}N$ nuclear quadrupole coupling constants, and electric dipole components of octopamine and synephrine are collected in Tables 1 and 2, respectively.

## RESULTS AND DISCUSSION

**Octopamine.** The predicted values of the rotational constants ($A$, $B$, and $C$) for the plausible conformers of octopamine (Table 1) indicate that the structures are near-prolate asymmetric rotors with sizable values of the $\mu_a$ component of the electric dipole moment. In a first survey of the microwave spectrum, we immediately identified two sets of $\mu_a$-type R-branch transitions appearing at $(B + C) \approx 1040$ MHz. They were assigned as corresponding to two rotamers, labeled I and II. As exemplified in Figure 3, all observed rotational transitions exhibited hyperfine structures, typically splitting each transition into three components. This hyperfine structure arises from the interaction between the electric


dx.doi.org/10.1021/jp4032223 | J. Phys. Chem. A 2013, 117, 4907−4915

**Table 1. Spectroscopic Parameters and Relative Energies Calculated at the MP2/6-311++G(d,p) Level of Theory for the Lowest-Energy Conformers of Octopamine**

| | $A^a$ | $B$ | $C$ | $\chi_{aa}$ | $\chi_{bb}$ | $\chi_{cc}$ | $\mu_a$ | $\mu_b$ | $\mu_c$ | $\Delta E^b$ | $\Delta G^c$ |
|---|---|---|---|---|---|---|---|---|---|---|---|
| $AG_{a1}$ | 3046.8 | 538.9 | 502.2 | 2.45 | −2.81 | 0.36 | −1.3 | 1.1 | −2.0 | 0 | 0 |
| $AG_{b1}$ | 3048.9 | 536.7 | 504.1 | 2.46 | −2.34 | −0.12 | −1.2 | 3.5 | −1.5 | 54 | 123 |
| $AG_{a2}$ | 3019.5 | 530.9 | 505.6 | 2.81 | −2.85 | −0.04 | 1.1 | 1.5 | 0.6 | 496 | 513 |
| $AG_{b2}$ | 3021.7 | 530.3 | 506.1 | 2.81 | −3.05 | 0.24 | 1.3 | 1.1 | 0.2 | 506 | 448 |
| $GG_{a1}$ | 2467.9 | 619.1 | 587.5 | 1.47 | −3.96 | 2.50 | 0.1 | 0.9 | −2.2 | 6 | 199 |
| $GG_{b1}$ | 2465.2 | 617.9 | 589.7 | 1.46 | −3.68 | 2.22 | −0.3 | −3.4 | −1.8 | 85 | 227 |
| $GG_{a2}$ | 2410.4 | 610.2 | 594.1 | −0.09 | 2.54 | −2.45 | −1.9 | 0.4 | −1.6 | 473 | 594 |
| $GG_{b2}$ | 2409.1 | 610.3 | 593.7 | −0.11 | 2.62 | −2.51 | −2.2 | −2.2 | 1.0 | 499 | 578 |

[a] $A$, $B$, and $C$ are rotational constants (in MHz); $\chi_{aa}$, $\chi_{bb}$, and $\chi_{cc}$ are elements of the $^{14}$N nuclear quadrupole coupling tensor (in MHz); and $\mu_a$, $\mu_b$ and $\mu_c$ are the electric dipole moment components (in D). [b] Relative energies with respect to the global minimum calculated at the MP2/6-311++G(d,p) level of theory (in cm$^{-1}$). [c] Gibbs energies calculated at 298 K at the MP2/6-311++G(d,p) level of theory (in cm$^{-1}$).

**Table 2. Spectroscopic Parameters and Relative Energies Calculated at the MP2/6-311++G(d,p) Level of Theory of the Lowest-Energy Conformers of Synephrine**

| | $A^a$ | $B$ | $C$ | $\chi_{aa}$ | $\chi_{bb}$ | $\chi_{cc}$ | $\mu_a$ | $\mu_b$ | $\mu_c$ | $\Delta E^b$ | $\Delta G^c$ |
|---|---|---|---|---|---|---|---|---|---|---|---|
| S-$AG_{a1}$ | 2596.0 | 418.5 | 387.9 | 2.61 | −2.93 | 0.32 | −1.6 | 0.8 | 2.0 | 50 | 21 |
| S-$AG_{b1}$ | 2599.9 | 417.2 | 389.0 | 2.62 | −2.60 | −0.03 | −1.7 | 3.3 | −1.3 | 103 | 117 |
| S-$AG_{a2}$ | 2361.9 | 395.6 | 389.1 | 2.87 | 0.54 | −3.42 | 1.0 | 0.9 | −1.1 | 472 | 393 |
| S-$AG_{b2}$ | 2367.7 | 394.9 | 389.5 | 2.87 | 0.60 | −3.47 | −1.3 | 0.7 | 1.1 | 483 | 331 |
| PS-$AG_{a1}$ | 2403.1 | 400.7 | 387.5 | 2.58 | −4.82 | 2.24 | −1.7 | 1.4 | −1.3 | 94 | 0 |
| PS-$AG_{b1}$ | 2408.6 | 398.4 | 389.4 | 2.59 | −4.71 | 2.12 | 1.7 | 3.6 | 0.3 | 145 | 133 |
| PS-$AG_{a2}$ | 2575.8 | 414.7 | 393.3 | 2.14 | 2.27 | −4.41 | −1.3 | −0.5 | 1.1 | 772 | 755 |
| PS-$AG_{b2}$ | 2587.6 | 414.1 | 393.4 | 2.14 | 2.28 | −4.42 | 1.4 | −2.1 | −1.9 | 793 | 707 |
| S-$GG_{a1}$ | 1729.0 | 498.0 | 471.2 | 1.77 | −0.76 | −1.00 | −0.3 | −2.2 | 0.5 | 0 | 173 |
| S-$GG_{b1}$ | 1726.0 | 497.8 | 472.1 | 1.75 | −0.40 | −1.35 | −0.2 | −3.0 | −2.3 | 76 | 202 |
| PS-$GG_{a1}$ | 1719.2 | 563.8 | 529.3 | 2.06 | −0.70 | −1.36 | 0.7 | 2.3 | 0.4 | 206 | 420 |
| PS-$GG_{b1}$ | 1715.6 | 564.3 | 530.3 | 2.05 | −0.54 | −1.51 | 0.1 | 2.9 | 2.3 | 289 | 383 |

[a] $A$, $B$, and $C$ are rotational constants (in MHz); $\chi_{aa}$, $\chi_{bb}$, and $\chi_{cc}$ are elements of the $^{14}$N nuclear quadrupole coupling tensor (in MHz); and $\mu_a$, $\mu_b$, and $\mu_c$ are the electric dipole moment components (in D). [b] Relative energies with respect to the global minimum calculated at the MP2/6-311++G(d,p) level of theory (in cm$^{-1}$). [c] Gibbs energies calculated at 298 K at the MP2/6-311++G(d,p) level of theory (in cm$^{-1}$).

**Table 3. Experimental Spectroscopic Parameters of the Four Observed Rotamers of Octopamine**

| | rotamer I | rotamer II | rotamer III | rotamer IV |
|---|---|---|---|---|
| $A^a$ | 3065.6858(11)[b] | 3064.85192(78) | 2479.83963(70) | 2478.4259(21) |
| $B$ | 540.46172(20) | 538.62660(18) | 614.51086(19) | 613.38156(16) |
| $C$ | 498.99506(17) | 501.10248(14) | 582.56681(33) | 584.25597(24) |
| $\chi_{aa}$ | 2.3300(70) | 2.3960(63) | 1.3220(75) | 1.257(35) |
| $\chi_{bb}$ | −2.9628(70) | −2.7624(76) | −3.7288(81) | −3.514(23) |
| $\chi_{cc}$ | 0.6328(70) | 0.3724(76) | 2.4068(81) | 2.257(23) |
| $\mu_a$[c] | Y | Y | N | N |
| $\mu_b$[c] | Y | Y | Y | Y |
| $\mu_c$[c] | Y | Y | N | Y |
| $N$[d] | 24 | 26 | 19 | 25 |
| $\sigma$[e] | 2.3 | 2.3 | 3.5 | 3.3 |

[a] $A$, $B$, and $C$ are the rotational constants (in MHz); $\chi_{aa}$, $\chi_{bb}$, and $\chi_{cc}$ are elements of the $^{14}$N nuclear quadrupole coupling tensor (in MHz). [b] Standard errors indicated in parentheses in units of the last digit. [c] Y (yes) and N (no) indicate whether *a*-, *b*-, and *c*-type transitions were observed for each structure. [d] Number of fitted transitions. [e] Root mean square of the fit (in kHz).

nuclear quadrupole of the $^{14}$N nucleus ($I$ = 1) present in the octopamine molecule and the molecular electric field gradient, coupling the nuclear spin with the overall rotation. Preliminary fittings and predictions allowed the measurement of $\mu_b$- and $\mu_c$-type R-branch transitions for both rotamers. Further scans under diverse experimental conditions were conducted to find lines belonging to other conformers. After the lines corresponding to rotamers I and II had been removed, two sequences of $\mu_b$-type R-branch transitions of the type $(J + 1)_{1,J+1} \leftarrow (J)_{0,J}$, corresponding to two new rotamers (labeled III and IV), were located. A total of eight and six $\mu_b$-type transitions were identified for rotamers III and IV, respectively. No lines assignable to other species could be found in the spectra.

The rotational spectrum of each rotamer was analyzed independently using a Watson rigid-rotor Hamiltonian in the $I^r$ representation,[17] $\mathbf{H}_R$, supplemented with an additional term, $\mathbf{H}_Q$, to account for the nuclear quadrupole coupling interaction,[18] which was set up in the coupled basis set (IJF), $\mathbf{I} + \mathbf{J} = \mathbf{F}$. The tensor describing the quadrupole coupling, $\boldsymbol{\chi}$, is


dx.doi.org/10.1021/jp4032223 | J. Phys. Chem. A 2013, 117, 4907−4915

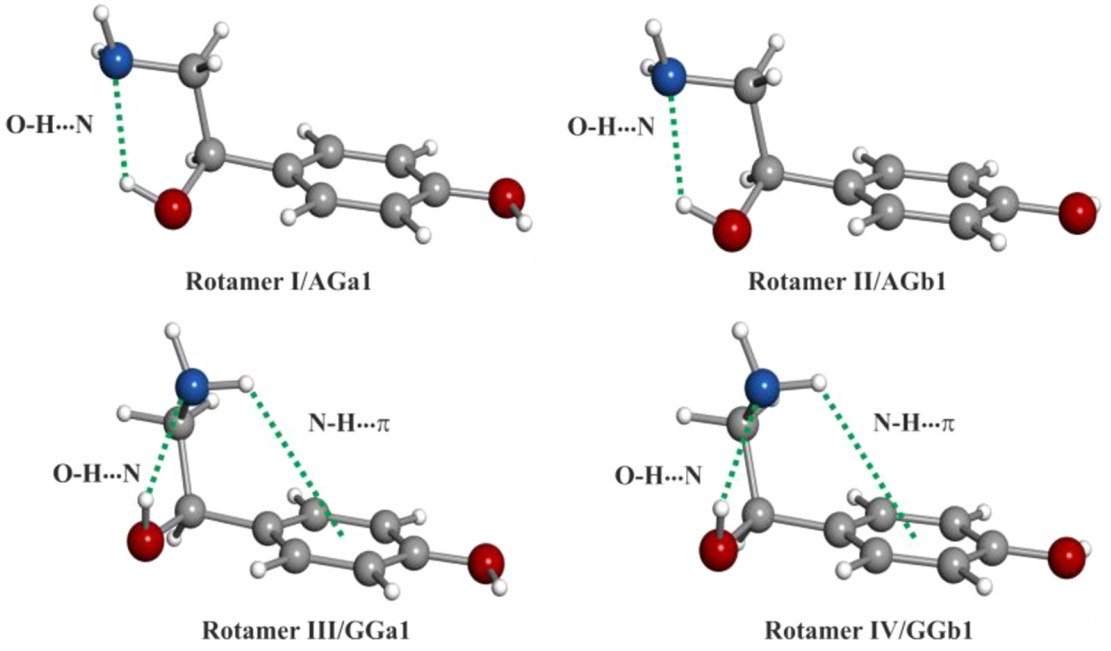


**Figure 4.** Four observed conformers of octopamine, showing the intramolecular interactions that stabilize the structures.

related to the molecular electrical field gradient tensor (at the $^{14}$N nucleus) **q**, by $\chi = eQ\mathbf{q}$, where $Q$ represents the $^{14}$N nuclear electric quadrupole moment. Only the diagonal elements of the nuclear quadrupole coupling tensor ($\chi_{aa}$, $\chi_{bb}$ and $\chi_{cc}$) were necessary to fit[19] the experimental frequencies within the estimated accuracy of the frequency measurements. The resulting spectroscopic constants for the four observed rotamers are reported in Table 3. All measured transitions are collected in Tables S1−S4 of the Supporting Information.

The conformational identification of the four observed rotamers was achieved by comparing the experimentally determined molecular properties reported in Table 3 with those predicted by ab initio calculations and provided in Table 1. The rotational constants provide information on the mass distribution of each rotamer and are normally conclusive in the conformational assignments. However, in the case of octopamine, the differences among rotational constants are not large enough to discriminate conformers. It is only possible to classify the observed rotamers as belonging to different families according to the values of the rotational constants. In turn, the quadrupole coupling constants are very sensitive to the chemical environment around the $^{14}$N nucleus and have been shown to be of extraordinary value in the identification of conformers of neurotransmitters,[2−4,6−10] usually allowing discrimination between species with very similar molecular shapes and, therefore, very similar rotational constants. However, as can be seen in Figure 1, the environment around the $NH_2$ group is nearly the same in all AG conformers. This fact is reflected in both the very similar values of the quadrupole coupling constants (Table 1) and the same observed hyperfine pattern (see Figure 3), thus precluding assignment of the conformers. Nevertheless, it is possible to use the predicted magnitudes of the dipole moment components in the assignment process.[5,10] The microwave power necessary for optimal polarization depends on the component of the dipole moment involved in a rotational transition. Indeed, the magnitudes of the dipole moment components correlate with the microwave power needed to optimally polarize the molecule; the higher the dipole moment components, the lower the microwave power needed. Hence, the difference in the values of the components of the conformers' dipole moments can be exploited to discriminate, in some favorable cases, between specific conformers, just by varying the polarization power. In the present case, the observation of relatively intense $\mu_c$-type R-branch transition lines for both rotamers I and II clearly revealed that these species must correspond to the $AG_{a1}/AG_{b1}$ pair of conformers, because the $AG_{a2}$ and $AG_{b2}$ forms have low $\mu_c$ dipole moment components. The only difference between the $AG_{a1}/AG_{b1}$ pair of conformers is the orientation of the phenolic OH group, which causes a large change in the $\mu_b$ dipole moment component (3.5 D for $AG_{b1}$ and 1.1 D for the $AG_{a1}$). Thus, the much lower power needed to polarize the $\mu_b$-type transition of rotamer II, compared to rotamer I, allows the identification of rotamer II as conformer $AG_{b1}$ and rotamer I as conformer $AG_{a1}$.

The experimental values of the rotational constants of the remaining rotamers, III and IV (Table 3), clearly indicate that they correspond to members of the GG family of conformers. As in the case of the AG-type conformers, the rotamers cannot be distinguished based solely on the values of the rotational constants. Conversely, in this case, the values of the quadrupole coupling constants ($\chi_{aa}$, $\chi_{bb}$, and $\chi_{cc}$) are sufficient to ascertain that rotamers III and IV correspond to the $GG_{a1}/GG_{b1}$ pair of conformers. However, once again, the distinction between the two conformers must be carried out in terms of the magnitudes of the dipole moment components and the microwave power needed to optimally polarize the molecules. Because the $\mu_b$-type transitions of rotamer IV require much less power to polarize than those of rotamer III, it can then be concluded that rotamer IV must correspond to conformer $GG_{b1}$, which exhibits a larger $\mu_b$ dipole moment component (3.4 D), whereas rotamer III can be assigned to form $GG_{a1}$ ($\mu_b$ = 0.9 D).

In conclusion, the four conformers of octopamine (Figure 4) were successfully identified through a comparison of the experimental rotational and quadrupole coupling constants with those predicted by ab initio calculations and by correlating


dx.doi.org/10.1021/jp4032223 | J. Phys. Chem. A 2013, 117, 4907−4915

the microwave power required to polarize rotational transitions with the predicted dipole moment components.

As noticed, the experimental determination of the $^{14}N$ quadrupole coupling constants constitutes an exceptional tool for the unequivocal establishment of the orientation of the side-chain $-NH_2$ group with respect to the molecular frame. These constants can be used to deduce the nature of the intramolecular interactions in which this functional group is involved. As can be seen in Figure 4, all of the detected conformers of octopamine share an intramolecular hydrogen bond of the O−H···N type as a common structural feature, similarly to what was found for the most stable conformers of the neurotransmitters norephedrine, ephedrine, and pseudoephedrine[4] and for other molecules containing vicinal OH and $NH_2$ groups.[20] The two observed AG-type conformers ($AG_{1a}$ and $AG_{1b}$) correspond to the most abundant species in the gas phase, in good agreement with the lowest predicted Gibbs energy values at the temperature and pressure prior to the expansion (Table 1), whereas the observed GG-type conformers ($GG_{1a}$ and $GG_{1b}$) correspond to the conformers with the third and fourth lowest Gibbs energies ($\Delta G^\circ$ = 199 and 227 $cm^{-1}$, respectively, compared with 0.0 and 123 $cm^{-1}$ for $AG_{1a}$ and $AG_{1b}$). On the other hand, the remaining four low-energy conformers of octopamine ($GG_{2a}$, $GG_{2b}$, $AG_{2a}$, and $AG_{2b}$, with predicted relative Gibbs energies above 440 $cm^{-1}$) share a weaker intramolecular hydrogen bond of the N−H···O type as a common structural feature. This general trend was also previously observed for other molecules bearing vicinal OH/$NH_2$ groups.[4,20] Note also that conformers GG, which contain a folded side chain, thus being less stabilized than the extended form, are stabilized to some extent through a weaker N−H···$\pi$ interaction between the amino group and the $\pi$ system of the aromatic ring. As in other neurotransmitters,[2−4,7−10] these N−H···$\pi$ interactions are also relevant in determining the relative stabilities of the different conformers of octopamine. Nevertheless, it can be concluded that the O−H···N interaction is clearly the dominant factor influencing the conformational preferences of the molecule.

The results obtained here for octopamine compare directly with those reported previously for APE.[15] For APE, two conformers were detected in the supersonic expansion: AG1 and GG1. Those correlate with the pairs of conformers (resulting from different orientations of the phenyl para-OH group) now observed for octopamine.

**Synephrine.** The experimental procedure followed for synephrine was an adaptation of that used for octopamine. Taking into account the predicted values of the $\mu_a$ electric dipole moment components listed in Table 2, scans were directed toward finding $\mu_a$-type R-branch transitions. Several sets of transitions corresponding to four different rotamers labeled I−IV were identified in the spectrum. Preliminary fittings[19] and predictions allowed the measurement of $\mu_b$- and $\mu_c$-type R-branch transitions for all of the species, with the exception of $\mu_c$-type lines for rotamer IV. Additional scans allowed identification of two sequences of $\mu_b$-type R-branch transitions of the type $(J+1)_{1,J+1} \leftarrow (J)_{0,J}$ for two new rotamers, labeled V and VI; $\mu_c$-type lines were added for rotamer VI but not for species V. As expected, all of the transitions found exhibited hyperfine structure, as shown in Figure 5. All measured rotational transitions are collected in Tables S5−S10 of the Supporting Information. A small number of weak signals remain unassigned in the wide frequency ranges scanned. They probably belong to other species of synephrine predicted to lie at higher energies. Because of the weakness of these lines and their insufficient number, it was not possible to attribute them to new rotamers.

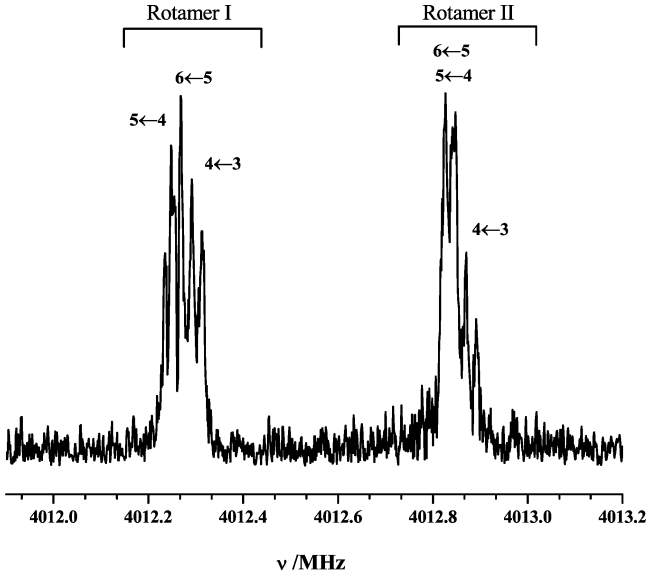


**Figure 5.** A section of the rotational spectrum of synephrine showing the $5_{05}−4_{04}$ rotational transition for rotamers I and II. The nuclear quadrupole hyperfine components are labeled with the quantum numbers F′ ← F″. The coaxial arrangement of the adiabatic expansion and resonator axes produces an instrumental Doppler doubling.

In the conformational assignment, it is possible to group the conformers in pairs as I/II, III/IV, and V/VI based on the rotational and quadrupole coupling constants provided in Table 4. The rotational constants of the first pair, I/II, resemble those theoretically predicted for the PS-$AG_{a1}$, PS-$AG_{b1}$, S-$AG_{a1}$, and S-$AG_{b1}$ conformers. However, one can quickly differentiate between the two families (PS and S) by comparing the observed quadrupole coupling constants of this pair of rotamers. Whereas the experimentally determined values for the $\chi_{aa}$ constant match both families reasonably well, the $\chi_{bb}$ and $\chi_{cc}$ elements allow one to conclude that rotamers I and II undoubtedly belong to the S-$AG_{a1/b1}$ pair and, moreover, can be ascribed to S-$AG_{a1}$ and S-$AG_{b1}$, respectively. This assignment is further confirmed by the optimum microwave power to polarize the $\mu_b$-type lines, which is much lower for rotamer II than for rotamer I, as predicted by the $\mu_b$ dipole moments ($AG_{a1}$, 0.8 D; $AG_{b1}$, 3.3 D). Second, based on their rotational constants, rotamers III and IV correspond to the other extended pairs PS-$AG_{a1}$/PS-$AG_{b1}$ and S-$AG_{a2}$/S-$AG_{b2}$. Once again, the determined values of the $\chi_{bb}$ and $\chi_{cc}$ constants allow identification of this pair as belonging to the PS-$AG_{a1/b1}$ conformer family. Given the low microwave power needed to polarize the $\mu_b$-type lines of rotamer IV, along with the absence of $\mu_c$-type R-branch transitions for this rotamer (but their presence for rotamer III), it is possible to assign rotamers III and IV to conformers PS-$AG_{a1}$ ($\mu_b$ = 1.4 D and $\mu_c$ = 1.3 D) and PS-$AG_{b1}$ ($\mu_b$ = 3.6 D and $\mu_c$ = 0.3 D), respectively. Using a similar approach in the analysis of the experimental data for rotamers V and VI, the rotational constants indicate that both belong to the S-GG family, and they can be distinguished on the basis of their electric dipole moments. Thus, rotamers V and VI were identified as S-$GG_{a1}$ and S-$GG_{b1}$, respectively.

Given the high resolution of the LA-MB-FTMW spectroscopic technique, independent analysis of the rotational spectra


dx.doi.org/10.1021/jp4032223 | J. Phys. Chem. A 2013, 117, 4907−4915

**Table 4. Experimental Spectroscopic Parameters of the Six Observed Rotamers of Synephrine**

| | rotamer I | rotamer II | rotamer III | rotamer IV | rotamer V | rotamer VI |
|---|---|---|---|---|---|---|
| $A^a$ | 2619.31951(91)[b] | 2621.43704(81) | 2431.79192(93) | 2429.8036(26) | 1751.6139(17) | 1749.29934(76) |
| $B$ | 417.815936(90) | 416.712685(80) | 401.522388(86) | 399.97472(24) | 491.43186(17) | 491.01374(10) |
| $C$ | 386.003079(87) | 387.043532(75) | 383.211109(81) | 385.16449(25) | 464.06642(12) | 465.271378(96) |
| $\chi_{aa}$ | 2.524(18) | 2.587(16) | 2.537(19) | 2.580(72) | 1.573(47) | 1.596(12) |
| $\chi_{bb}$ | −3.054(13) | −2.778(12) | −4.767(15) | −4.764(62) | −1.187(31) | −0.9142(93) |
| $\chi_{cc}$ | 0.530(13) | 0.250(12) | 2.231(14) | 2.184(62) | −0.387(31) | −0.6818(93) |
| $\mu_a^c$ | Y | Y | Y | Y | N | N |
| $\mu_b^c$ | Y | Y | Y | Y | Y | Y |
| $\mu_c^c$ | Y | Y | Y | N | N | Y |
| $N^d$ | 31 | 32 | 18 | 20 | 14 | 20 |
| $\sigma^e$ | 2.1 | 1.8 | 2.3 | 3.1 | 1.7 | 2.1 |

[a] $A$, $B$, and $C$ are the rotational constants (in MHz); $\chi_{aa}$, $\chi_{bb}$, and $\chi_{cc}$ are elements of the $^{14}$N nuclear quadrupole coupling tensor (in MHz). [b] Standard errors indicated in parentheses in units of the last digit. [c] Y (yes) and N (no) indicate whether *a*-, *b*-, and *c*-type transitions were observed for each structure. [d] Number of fitted transitions. [e] Root mean square of the fit (in kHz).

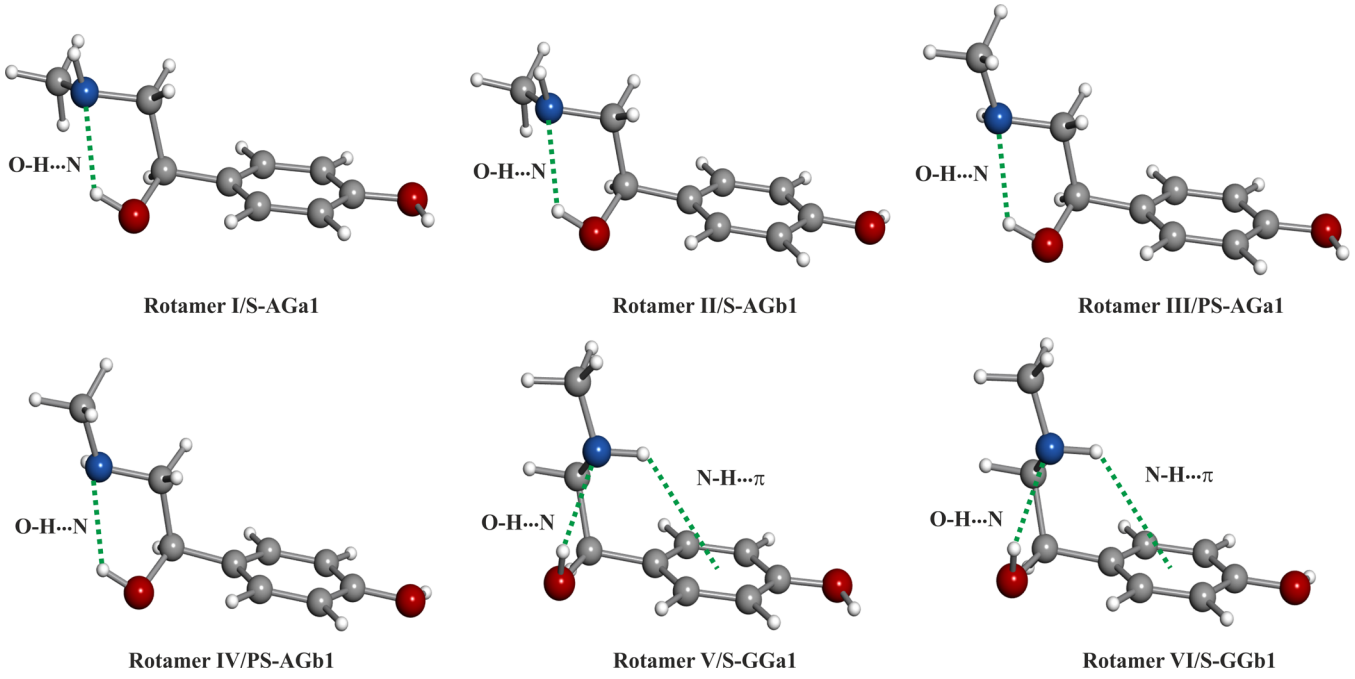


**Figure 6.** Six observed conformers of synephrine, showing the intramolecular interactions that stabilize the structures.

of individual conformers becomes possible, thus leading to the conclusive assignment of six different conformers of synephrine, in contrast to the previously reported study on the same molecule using electronic spectroscopy.[14] In that work, hole-burning spectra were interpreted in terms of the coexistence of six conformers in the molecular beam, classified into three groups based on spectral similarity. The two groups originated from the two different orientations of the phenolic OH group. They assigned conformational geometries by comparing the experimental and theoretical IR spectra, except for the orientation of the phenolic OH group.

As can be seen from Figure 6, all detected forms of synephrine are stabilized by an O−H···N bond between the lone electron pair of the N atom and the hydroxyl group of the side chain, thus following the trend already noticed for octopamine. Also as in octopamine, conformers bearing a N−H···O hydrogen bond follow in order of increasing energy those with the dominant O−H···N stabilizing interaction, and conformers of the S-GG type, with a folded side chain, present an extra N−H···$\pi$ hydrogen-bond-type interaction between the amino group and the $\pi$ system of the aromatic ring. On the other hand, steric hindrance induced by the methylamino moiety precludes this side chain from interacting favorably with the $\pi$ system of the aromatic ring, thus preventing further stabilization and leading to an increase in the conformer relative energies, for instance, in the case of the PS-GG family of conformers. Indeed, one could expect, by comparison with octopamine, for which four conformers were detected, that eight conformers of synephrine could be observed: one S and one PS conformer per octopamine conformer detected. However, that is not the case, because members of the PS-GG family have higher relative energies.

As for octopamine, these results for synephrine can be contrasted with those reported for the analogue molecule MAPE, for which $AG_{1a}$, $AG_{1b}$, and $GG_{1a}$ conformers where found in the gas phase.[15] In this case, there is also a doubling of the number of conformers in synephrine with respect to MAPE, resulting from the different orientations of the phenyl para-OH group.


dx.doi.org/10.1021/jp4032223 | J. Phys. Chem. A 2013, 117, 4907−4915

## CONCLUSIONS

In summary, the present study has probed the conformational landscape of the neurotransmitters octopamine and synephrine by rotational spectroscopy. Interpretation of the experimental results was supported by an extensive series of theoretical calculations on the two molecules performed at the MP2/6-311++G(d,p) level of approximation. Four conformers of octopamine and six conformers of synephrine were identified experimentally. The observed species of both molecules correspond to the predicted most-abundant conformers, each of them being characterized by a strongly stabilizing O−H···N intramolecular hydrogen bond.

This investigation can contribute to an improved understanding of the role of intramolecular forces in the conformational preferences of neurotransmitters.

## ASSOCIATED CONTENT

### Supporting Information

List of measured transitions for all of the observed conformers of octopamine and synephrine. This material is available free of charge via the Internet at http://pubs.acs.org.

## AUTHOR INFORMATION

### Corresponding Author

*E-mail: jlalonso@qf.uva.es. Phone: +34 983186348. Fax: +34 983186349.

### Notes

The authors declare no competing financial interest.

## ACKNOWLEDGMENTS

This research was supported by the Ministerio de Ciencia y Innovación (Grant CTQ 2010-19008), Consolider Ingenio 2010 (CSD 2009-00038), Junta de Castilla y León (VA070A08), and Spain-Portugal Bilateral Project AIB2010PT-00315. C.B. thanks Ministerio de Ciencia e Innovación for the FPI Grant (BES-2011-047695). R.F. and A.S. acknowledge Fundação para a Ciência e a Tecnologia (FCT, Lisbon, Portugal; Project PTDC/QUI-QUI/111879/2009 and Doctoral Grant SFRH/BD/44443/2008, also funded by COMPETE-QREN-EU).

## REFERENCES

(1) (a) Majumdar, D.; Guha, S. Conformation, Electrostatic Potential and Pharmacophoric Pattern of GABA (γ-Aminobutyric Acid) and Several GABA Inhibitors. *J. Mol. Struct. (THEOCHEM)* **1988**, *180*, 125−140. (b) Goldberg, N. R.; Beuming, T.; Soyer, O. S.; Goldstein, R. A.; Weinstein, H.; Javitch, J. A. Probing Conformational Changes in Neurotransmitter Transporters: A Structural Context. *Eur. J. Pharmacol.* **2003**, *479* (1−3), 3−12. (c) Zhao, Y.; Terry, D.; Shi, L.; Weinstein, H.; Blanchard, S. C.; Javitch, J. A. Single-Molecule Dynamics of Gating in a Neurotransmitter Transporter Homologue. *Nature* **2010**, *465* (7295), 188−193.

(2) López, J. C.; Cortijo, V.; Blanco, S.; Alonso, J. L. Conformational Study of 2-Phenylethylamine by Molecular-Beam Fourier Transform Microwave Spectroscopy. *Phys. Chem. Chem. Phys.* **2007**, *9* (32), 4521−4527.

(3) Cortijo, V.; Alonso, J. L.; López, J. C. The Conformational Landscape of *p*-Methoxyphenylethylamine from Molecular Beam Fourier Transform Microwave Spectroscopy. *Chem. Phys. Lett.* **2008**, *466* (4−6), 214−218.

(4) Alonso, J. L.; Sanz, M. E.; López, J. C.; Cortijo, V. Conformational Behavior of Norephedrine, Ephedrine, and Pseudoephedrine. *J. Am. Chem. Soc.* **2009**, *131* (12), 4320−4326.

(5) (a) Alonso, J. L.; Pérez, C.; Sanz, M. E.; López, J. C.; Blanco, S. Seven Conformers of L-Threonine in the Gas Phase: A LA-MB-FTMW Study. *Phys. Chem. Chem. Phys.* **2009**, *11* (4), 617−627. (b) Peña, I.; Sanz, M. E.; López, J. C.; Alonso, J. L. Preferred Conformers of Proteinogenic Glutamic Acid. *J. Am. Chem. Soc.* **2012**, *134*, 2305−2312.

(6) Cortijo, V.; Sanz, M. E.; Lopez, J. C.; Alonso, J. L. Conformational Study of Taurine in the Gas Phase. *J. Phys. Chem. A* **2009**, *113* (52), 14681−14683.

(7) Alonso, J. L.; Cortijo, V.; Mata, S.; Pérez, C.; Cabezas, C.; López, J. C.; Caminati, W. Nuclear Quadrupole Coupling Interactions in the Rotational Spectrum of Tryptamine. *J. Mol. Spectrosc.* **2011**, *269* (1), 41−48.

(8) Blanco, S.; López, J. C.; Mata, S.; Alonso, J. L. Conformations of γ-Aminobutyric Acid (GABA): The Role of the $n-\pi$ Interaction. *Angew. Chem., Int. Ed.* **2010**, *49* (48), 9187−9192.

(9) Cabezas, C.; Varela, M.; Peña, I.; López, J. C.; Alonso, J. L. The Microwave Spectrum of Neurotransmitter Serotonin. *Phys. Chem. Chem. Phys.* **2012**, *14* (39), 13618−13623.

(10) Cabezas, C.; Peña, I.; López, J. C.; Alonso, J. L. Seven Conformers of Neutral Dopamine Revealed in the Gas Phase. *J. Phys. Chem. Lett.* **2013**, *4* (3), 486−490.

(11) (a) Livingstone, M. S.; Harris-Warrick, R. M.; Kravitz, E. A. Serotonin and Octopamine Produce Opposite Postures in Lobsters. *Science* **1980**, *208* (4439), 76−79. (b) Zhou, C.; Rao, Y.; Rao, Y. A Subset of Octopaminergic Neurons are Important for Drosophila Aggression. *Nat. Neurosci.* **2008**, *11* (9), 1059−1067.

(12) (a) Wheaton, T. A.; Stewart, I. The Distribution of Tyramine, *N*-Methyltyramine, Hordenine, Octopamine, and Synephrine in Higher Plants. *Lloydia* **1970**, *33* (2), 244−54. (b) Vieira, S. M.; Karine, H. T.; Glória, M. B. A. Profile and Levels of Bioactive Amines in Orange Juice and Orange Soft Drink. *Food Chem.* **2007**, *100*, 895−903.

(13) Rossato, L. G.; Costa, V. M.; Limberger, R. P.; Bastos, M. d. L.; Remião, F. Synephrine: From Trace Concentrations to Massive Consumption in Weight Loss. *Food Chem. Toxicol.* **2011**, *49* (1), 8−16.

(14) Ishiuchi, S.; Asakawa, T.; Mitsuda, H.; Miyazaki, M.; Chakraborty, S.; Fujii, M. Gas-Phase Spectroscopy of Synephrine by Laser Desorption Supersonic Jet Technique. *J. Phys. Chem. A* **2011**, *115* (37), 10363−10369.

(15) Melandri, S.; Ragno, S.; Maris, A. Shape of Biomolecules by Free Jet Microwave Spectroscopy: 2-Amino-1-phenylethanol and 2-Methylamino-1-phenylethanol. *J. Phys. Chem. A* **2009**, *113* (27), 7769−7773.

(16) Frisch, M. J.; Trucks, G. W.; Schlegel, H. B.; Scuseria, G. E.; Robb, M. A.; Cheeseman, J. R.; Scalmani, G.; Barone, V.; Mennucci, B.; Petersson, G. A.; Nakatsuji, H.; Caricato, M.; Li, X.; Hratchian, H. P.; Izmaylov, A. F.; Bloino, J.; Zheng, G.; Sonnenberg, J. L.; Hada, M.; Ehara, M.; Toyota, K.; Fukuda, R.; Hasegawa, J.; Ishida, M.; Nakajima, T.; Honda, Y.; Kitao, O.; Nakai, H.; Vreven, T.; Montgomery, J. A., Jr.; Peralta, J. E.; Ogliaro, F.; Bearpark, M.; Heyd, J. J.; Brothers, E.; Kudin, K. N.; Staroverov, V. N.; Keith, T.; Kobayashi, R.; Normand, J.; Raghavachari, K.; Rendell, A.; Burant, J. C.; Iyengar, S. S.; Tomasi, J.; Cossi, M.; Rega, N.; Millam, J. M.; Klene, M.; Knox, J. E.; Cross, J. B.; Bakken, V.; Adamo, C.; Jaramillo, J.; Gomperts, R.; Stratmann, R. E.; Yazyev, O.; Austin, A. J.; Cammi, R.; Pomelli, C.; Ochterski, J. W.; Martin, R. L.; Morokuma, K.; Zakrzewski, V. G.; Voth, G. A.; Salvador, P.; Dannenberg, J. J.; Dapprich, S.; Daniels, A. D.; Farkas, Ö.; Foresman, J. B.; Ortiz, J. V.; Cioslowski, J.; Fox, D. J. *Gaussian 09*, revision B.01; Gaussian, Inc.: Wallingford, CT, 2010.

(17) Watson, J. K. G. In *Vibrational Spectra and Structure*; Durig, J. R., Ed.; Elsevier: Amsterdam, 1977; Vol. *6*, pp 1−89.

(18) Gordy, W.; Cook, R. L. *Microwave Molecular Spectra*, 3rd ed.; Techniques of Chemistry Series; John Wiley & Sons: New York, 1984; Vol. *XVIII*.

(19) Pickett, H. M. The Fitting and Prediction of Vibration-Rotation Spectra with Spin Interactions. *J. Mol. Spectrosc.* **1991**, *148*, 371−377.

(20) (a) Silva, C. F. P.; Duarte, M. L. T. S.; Fausto, R. A Concerted SCF-MO Ab Initio and Vibrational Spectroscopic Study of the Conformational Isomerism in 2-Aminoethanol. *J. Mol. Struct.* **1999**, *482/483*, 591−599. (b) Cacela, C.; Fausto, F.; Duarte, M. L. A Combined Matrix-Isolation Spectroscopy and MO Study of 1-Amino-2-propanol. *Vib. Spectrosc.* **2001**, *26*, 113−131. (c) Fausto, F.; Cacela, C.; Duarte, M. L. Vibrational Analysis and Structural Implications of H-Bonding in Isolated and Aggregated 2-Amino-1-propanol: A Study by MI-IR and Raman Spectroscopy and Molecular Orbital Calculations. *J. Mol. Struct.* **2000**, *550/551*, 365−388.